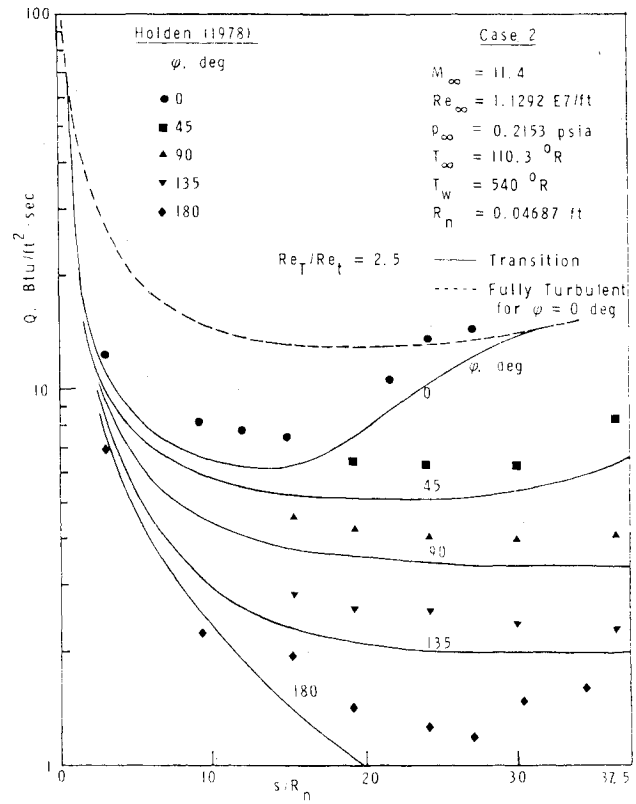

Fig. 2 Surface heat-transfer distribution ($\alpha = 2.93$ deg).

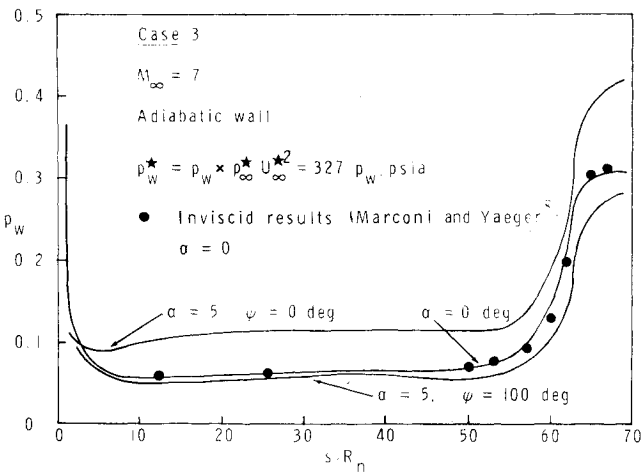

Fig. 3 Spike inlet surface pressure distribution ($\alpha = 0$ and 5 deg).

ratio ($\bar{x}$) of transition end-to-onset boundary-layer-edge Reynolds number is assumed to be 2.5. It is noted that the comparison is in reasonably good agreement, within 15% difference for all the planes (from windward side $\phi = 0$ to leeward side $\phi = 180$).

Figure 3 shows the surface pressure distribution from part of a spike inlet diffuser which is a spherically blunted cone with three different isentropic compression sections downstream of the cone at different Mach numbers and angles of attack. For the axisymmetric solutions ($\alpha = 0$ deg), the surface pressure increased from 19.63 psia in the cone region to 91.60 psia at the end of the compression region. For the angle-of-attack case in the windward plane ($\phi = 0$ deg), the surface pressure increased to 137.40 psia at the end of compression. The inviscid solutions from Marconi and Yaeger[8] are also presented and are in very good agreement with the viscous shock-layer calculations.

Conclusion

Numerical solutions for the three-dimensional viscous shock-layer equations for laminar, transitional, and/or turbulent flows are presented. The present solutions for both laminar and turbulent flows are in good agreement with boundary-layer solutions. The results clearly show the higher-order boundary-layer effects. The heating rate is approximately 15% lower than the experimental data. It is not clear why the experimental data are higher than the prediction. Equilibrium real-gas effects do not appear to be the cause, since the wind-tunnel conditions are essentially perfect gas.

References

[1] Anderson, E.C. and Lewis, C.H., "Laminar or Turbulent Boundary-Layer Flow of Perfect Gases or Reacting Gas Mixtures in Chemical Equilibrium," NASA CR-1893, Oct. 1971.

[2] Murray, A.L. and Lewis, C.H., "Hypersonic Three-Dimensional Viscous Shock-Layer Flow over Blunt Bodies," *AIAA Journal,* Vol. 16, Dec. 1978, pp. 1279-1286.

[3] Anderson, C.E. and Moss, J.N., "Numerical Solution of the Steady State Navier-Stokes Equations for Hypersonic Flow About Blunt Axisymmetric Bodies," NASA TM-71977, June 1974.

[4] Cebeci, T., "Behavior of Turbulent Flows near a Porous Wall with Pressure Gradient," *AIAA Journal,* Vol. 3, Dec. 1970, pp. 2152-2156.

[5] Dhawan, S. and Narasimha, R., "Some Properties of Boundary Layer Flow During the Transition from Laminar to Turbulent Motion," *Journal of Fluid Mechanics,* Vol. 3, Pt. 4, Jan. 1958, pp. 418-436.

[6] Szema, K.Y. and Lewis, C.H., "Three-Dimensional Hypersonic Laminar, Transitional and/or Turbulent Flows," AIAA Paper 80-1457, July 1980.

[7] Holden, M.S., "Study of the Effects of Transitional and Turbulent Boundary Layer on the Aerodynamic Performance of Hypersonic Reentry Vehicle in High Reynolds Number Flows," Calspan Rept. AB-5834-4-2, Dec. 1978.

[8] Marconi, F. and Yaeger, L., "Development of a Computer Code for Calculating the Steady Super/Hypersonic Inviscid Flow around Real Configurations," NASA CR-2675, April 1976.

AIAA 82-4043

Effect of Radial Fins on Base Drag of an Axisymmetric Body at Low Speeds

Kamlesh Kapoor*
Indian Institute of Technology, Bombay, India

Introduction

It is well known that the total drag of an axisymmetric blunt based body of revolution, in general, consists of friction, wave, and base drag. It is the aim of the designer to eliminate or as far as possible minimize these retarding forces. Whereas the friction drag is essentially a function of the wetted area and the local Reynolds number, wave drag and base drag are strongly dependent on the shape of the vehicle. It is usually not possible to completely eliminate the base area on a missile/rocket or any other streamlined vehicle because of the necessity to accommodate the propulsion system and other related equipment in the base region. At low speeds, the base drag forms a major part of the total drag.

The axisymmetric base flow problem at low speeds has been a subject of study in recent years. References 1-6 represent

Received May 12, 1980; revision received April 9, 1981.

*Project Engineer, Department of Aeronautical Engineering.

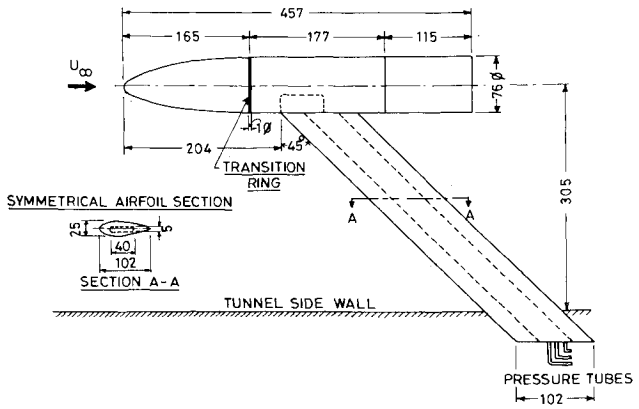

Fig. 1 The experimental model.

some of the experimental investigations of the phenomenon. The investigation of Merz et al.[6] has particularly studied, in detail, the development of the near-wake region of a blunt based body of revolution. In regard to base flow control with a view to reduce the base drag, the first experiments were due to Mair.[7] These investigations showed that the base drag could be reduced by mounting a rear disk on the base. Later, Mair[8] with boattailed afterbodies, Morel with base cavities[9] and base slant,[10] and recently Gai and Kapoor[11] with a jet issuing from the base, have achieved reduction in the base drag. Another interesting work on base flow control has been reported by Goodyer.[12] He introduced certain geometrical modifications to the base in the form of slits. Surprisingly, the base drag was increased. Gai and Patil[13] have also shown that devices like slits and trailing-edge serrations,[14,15] which are very effective in reducing the base drag in two-dimensional flow, are not necessarily effective in the case of three-dimensional blunt body wakes. In view of these available data, an experimental investigation was carried out to study the effect of radial fins on the base drag of an axisymmetric body.

Experimental Apparatus and Technique

The basic model used for tests is shown in Fig. 1. In ellipsoidal nosed axisymmetric blunt based model of fineness ratio 6, incorporating different base modifications was used for the experiments. The model, supported rigidly by a strut, was mounted on one of the side walls of the test section in such a way that the model was at the center of the tunnel at zero incidence. In addition to the blunt base, five different base configurations of radial fins were used and are shown in Fig. 2. Configurations a and b have two splitter plates perpendicular to each other of lengths equal to the base diameter and half of the base diameter, respectively. Configurations c and d have four radial fins, which are 25 mm in breadth and have lengths equal to the base diameter and half of the base diameter, respectively. Configuration e has eight radial fins of 25 mm breadth and length equal to the base diameter. All radial fins are 5 mm in thickness. All configurations were provided with 24 pressure taps, 12 each, equally spaced on two circles of radii 15 and 31 mm.

This experimental investigation was conducted in an open-circuit low-speed wind tunnel with a closed working section of a square cross section of 610×610 mm, at a freestream velocity of 25 m/s. The Reynolds number based on the free-stream conditions and the base diameter was 1.24×10^5. Corrections for solid and wake blockage were considered and these were estimated to be about 0.5% for solid blockage and 1.37% for wake blockage. Since these corrections were considered quite small, no corrections for blockage have been made in presenting the results. Throughout, the pressure measurements were made using a projection manometer which has an accuracy of ± 0.1 mm of alcohol. This gives an

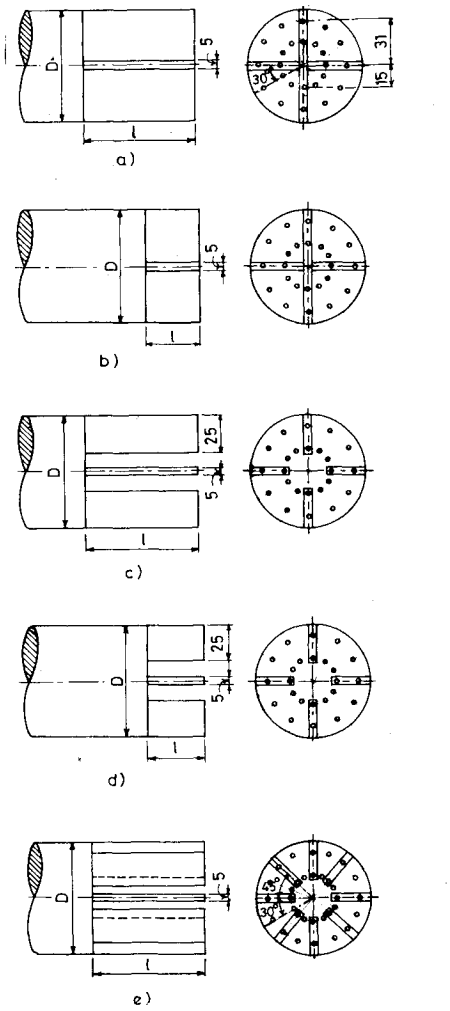

a) BASE WITH TWO SPLITTER PLATES OF l = D
b) BASE WITH TWO SPLITTER PLATES OF l = D/2
c) FOUR RADIAL FINS OF l = D
d) FOUR RADIAL FINS OF l = D/2
e) EIGHT RADIAL FINS OF l = D
D = 76 mm

Fig. 2 Different base geometries.

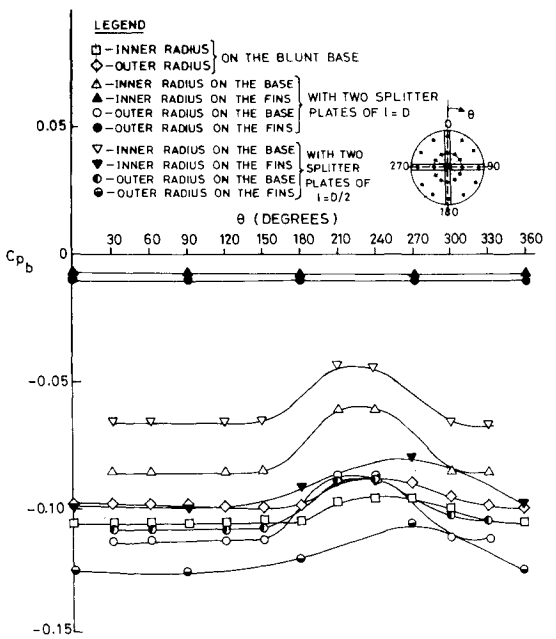

Fig. 3 Base pressures on the base with two splitter plates.

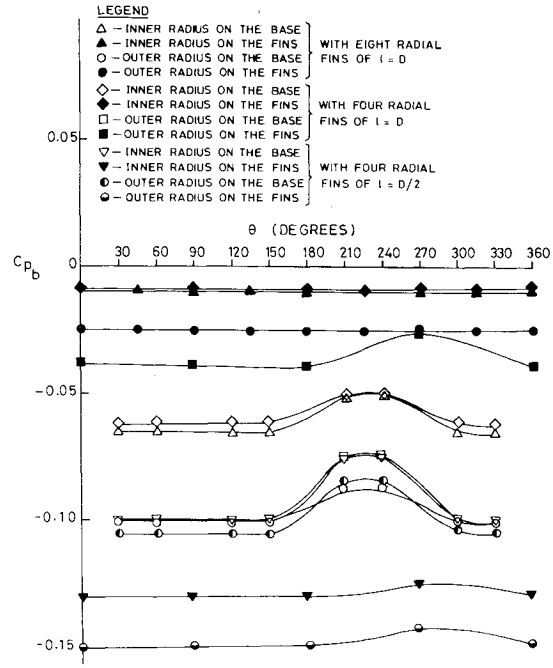

Fig. 4 Base pressures on the base with radial fins.

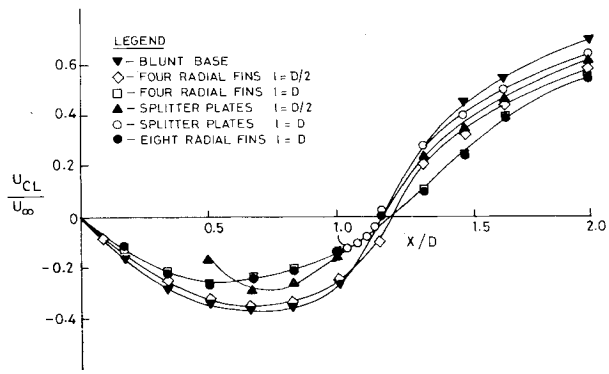

Fig. 5 Velocity distribution along near-wake centerline.

overall accuracy of ±0.003 in pressure coefficient. A special probe[13] was used to locate the reattachment point (rear stagnation point) in the recirculation zone behind the base.

The reference pressure for normalizing the base pressure has been taken at two diameters ahead of the base.[13]

Results and Discussion

The effect of radial fins on the base pressure is shown in Figs. 3 and 4. It is observed that the base pressures are not uniform. The pressures are somewhat higher in the range of 180 deg $\leq \theta \leq$ 300 deg. This could not be due to the strut effect, as the strut location corresponds to $\theta = 90$ deg. Similar types of nonuniform pressure distribution have also been observed by Mair and Wilkin.[16] They have surmised that such a nonuniformity is always found whenever the axisymmetric body is at very small yaw (usually < 0.75 deg). It is interesting to observe that the radial fins do affect the radial pressure distribution on the base. The pressures are lower on the outer radii and are higher on the inner radii. This is just contrary to what has been observed on the blunt base. This observation suggests that the radial fins affect the basic flowfield behind the axisymmetric bodies. The lengths of the radial fins are seen to be important as far as base drag reduction is concerned. The base pressures on the radial fins are increased when the length of the fins is increased from $D/2$ to D. The overall base drag is decreased appreciably. When the central portion of radial fins is removed, the results show that the base drag is further decreased. There is no appreciable effect of number of fins on the base drag as is evident from the results, when the number of fins is increased from 4 to 8. The comparison of the effectiveness of various radial fins is shown in Table 1. The mean value of base pressure coefficient, in each case, has been calculated by taking into account the pressure acting on the base as well as on the fins and their respective areas.

Table 1 Comparison of effectiveness of various radial fins on the base drag of axisymmetric bodies

Type of base	C_{pb}	Reduction of base drag with reference to the blunt base, %
Blunt base	−0.103	–
Splitter plates, $l = D$	−0.088	14.6
Splitter plates, $l = D/2$	−0.093	9.7
Four radial fins, $l = D$	−0.074	28.2
Four radial fins, $l = D/2$	−0.013	0
Eight radial fins, $l = D$	−0.072	30.0

Figure 5 shows the velocity distribution along the near-wake centerline. It is clear from the figure that a closed bubble with a recirculation zone is formed behind the base for all radial fins. The maximum negative velocity in the bubble is around 35% of freestream velocity and is in agreement with the data of Merz et al.[6] for blunt bases. It should be noted that the location of the rear stagnation point is almost the same for all the models tested. This was found to be about 1.2 times the base diameter downstream from the base. The negative velocities were found to be decreased in the presence of radial fins, depending upon their size and shape. The reduction in negative velocities is associated with the corresponding reduction of base drag of various models tested.

Conclusions

The following are the major conclusions of the present study:

1) With radial fins, the base pressures are higher on the inner portion and lower on the outer portion of the base.

2) Length of the radial fin is important. When fin length was increased to the base diameter, the base drag was decreased appreciably.

3) The negative velocities are decreased in the recirculation zone when radial fins are introduced to the base.

4) The location of rear stagnation point was found to be almost the same for all the radial fins.

References

[1] Calvert, J.R., "Experiments on Low Speed Flow Past Cones," *Journal of Fluid Mechanics*, Vol. 27, Part 2, 1967, pp. 273-289.

[2] Badri Narayanan, M.A., "Some Investigations on Base Flow Behind Cylindrical Bodies in Incompressible Flow," *Journal of the Aeronautical Society of India*, Vol. 25, May 1973, pp. 67-72.

[3] Eldred, K.M., "Base Pressure Fluctutions," *Journal of the Acoustical Society of America*, Vol. 33, Jan. 1961, pp. 59-63.

[4] Merz, R.A., "Subsonic Base Pressure Fluctuations," *AIAA Journal*, Vol. 17, April 1979, pp. 436-437.

[5] Merz, R.A., Page, R.H., and Przirembel, C.E.G., "Rear Stagnation Point Location in a Subsonic Near Wake," *Journal of Spacecraft and Rockets*, Vol. 13, May 1976, pp. 319-320.

[6] Merz, R.A., Page, R.H., and Przirembel, C.E.G., "Subsonic Axisymmetric Near Wake Studies," *AIAA Journal*, Vol. 16, July 1978, pp. 656-662.

[7] Mair, W.A., "The Effect of a Rear Mounted Disc on the Drag of a Blunt Based Body of Revolution," *The Aeronautical Quarterly*, Vol. 16, Nov. 1965, pp. 350-360.

[8] Mair, W.A., "Reduction of Base Drag by Boattailed After Bodies in Low Speed Flow," *The Aeronautical Quarterly*, Vol. 20, Nov. 1969, pp. 307-320.

[9]Morel, T., "Effect of Base Cavities on the Aerodynamic Drag of an Axisymmetric Cylinder," *The Aeronautical Quarterly,* Vol. 30, May 1979, pp. 400-412.
[10]Morel, T., "Effect of Base Slant on Flow in Near Wake of an Axisymmetric Cylinder," *The Aeronautical Quarterly,* Vol. 31, May 1980, pp. 132-147.
[11]Gai, S.L. and Kapoor, K., "The Near Wake of a Blunt Based Body of Revolution in the Pressure of Jet Issuing from the Base," *Proceedings of the First Asian Congress of Fluid Mechanics,* Dec. 1980, Bangalore, India.
[12]Goodyer, M.J., "Some Experimental Investigations into the Drag Effect of Modifications to the Blunt Base of a Body of Revolution," Institute of Sound and Vibration, Rept. 150, Univ. of Southampton, England, July 1966.
[13]Gai, S.L. and Patil, S.R., "Subsonic Axisymmetric Base Flow Experiments with Base Modifications," *Journal of Spacecraft and Rockets,* Vol. 17, Jan. 1980, pp. 42-46.
[14]Tanner, M., "A Method of Reducing the Base Drag of Wings with Blunt Trailing Edges," *The Aeronautical Quarterly,* Vol. 23, Feb. 1972, pp. 15-22.
[15]Tanner, M., "Reduction of Base Drag," *Progress in Aerospace Sciences,* Vol. 16, No. 4, 1975, pp. 369-374.
[16]Mair, W.A. and Wilkin, S.M., "Asymmetric Distribution of Base Pressure on an Axisymmetric Body," *The Aeronautical Journal,* June 1978, pp. 273-275.

AIAA 82-4044

Thermal Decomposition Kinetics of Polybutadiene Binders

K.N. Ninan* and K. Krishnan†
Vikram Sarabhai Space Centre, Trivandrum, India

Introduction

THE thermal decomposition of polymeric fuel binders plays an important role in the combustion of solid propellants.[1,2] Thermogravimetry (TG) has been extensively used for the determination of the thermal decomposition kinetics of polymers.[3] The kinetic parameters (energy of activation, E, and preexponential factor, A) calculated from TG curves are affected, in certain cases, by procedural factors like heating rate and sample mass.[4] The effect of heating rate on the pyrolysis of binders has been described.[5] It is, therefore, necessary to establish the effect of the procedural factors on E and A of the binder decomposition, for any meaningful correlation of the kinetic parameters with propellant combustion. Carboxyl and hydroxyl terminated polybutadienes (CTPB and HTPB) are used as binders for modern solid propellants. In this investigation, we have attempted to study the effect of the procedural factors, the functional groups, and the method of polymerization on the kinetics of their thermal decomposition.

Experimental

Samples

Three CTPB and two HTPB resins, obtained from different sources and prepared by different methods (free radical and anionic polymerization), were used in the study and their details are shown in Table 1.

Received Dec. 16, 1980; revision received July 21, 1981.

*Head, Analytical and Spectroscopy Division, Propellants, and Chemicals Group.
†Scientist, Analytical and Spectroscopy Division, Propellants, and Chemicals Group.

Table 1 Details of resins used in the study

Code	Type of resin	Method of preparation	Source
ISRO-CTPB	CTPB	Free radical	VSSC, India
HC-434	CTPB	Free radical	Thiokol, U.S.A.
Butarez CTL	CTPB	Anionic	Phillips, U.S.A.
ISRO-HTPB	HTPB	Free radical	VSSC, India
Butarez HTS	HTPB	Anionic	Phillips, U.S.A.

TG Experiments

The TG experiments were carried out with DuPont 990 Thermal Analyzer in an atmosphere of dry nitrogen purged at a flow rate of 50 $cm^3\ min^{-1}$. Seven heating rates (1, 2, 5, 10, 20, 50, and 100°C min^{-1}) at a constant sample mass (5 ± 0.1 mg) and seven sample masses (1, 2.5, 5, 7.5, 10, 15, and 20 mg) at a constant heating rate (10°C min^{-1}) were employed. Since heating rate has a more pronounced effect on the kinetic parameters,[4] the TG curves of all five samples were taken at the seven heating rates. The effect of sample mass was studied only for HC-434.

Results and Discussion

The kinetic parameters were calculated using three well-known integral equations[4]:

1) Coats-Redfern equation

$$\ell n\left(\frac{1-(1-\alpha)^{1-n}}{(1-n)T^2}\right)=\ell n\left[\frac{AR}{\phi E}\left(1-\frac{2RT}{E}\right)\right]-\frac{E}{RT}$$

2) MacCallum-Tanner equation

$$\log\left(\frac{1-(1-\alpha)^{1-n}}{1-n}\right)=\log\left(\frac{AE}{\phi R}\right)-0.483\,E^{0.435}-\frac{(0.449+0.217E)\times 10^3}{T}$$

3) Horowitz-Metzger equation

$$\ell n\left(\frac{1-(1-\alpha)^{1-n}}{1-n}\right)=\ell n\left(\frac{ART_s^2}{\phi E}\right)-\frac{E}{RT_s}+\frac{E\theta}{RT_s^2}$$

[where $g(\alpha)=(1-(1-\alpha)^{1-n})/(1-n)$, α = fraction decomposed, n = order parameter, T = temperature (K), ϕ = heating rate, R = gas constant, T_s = DTG peak temperature, and $\theta = T - T_s$].

The order parameter was evaluated with the Coats-Redfern equation. Using a computer, linear plots of $\ell n(g(\alpha)/T^2)$ vs $1/T$ were drawn by the method of least squares for different values of n in the range 0 to 2 and the order parameter was obtained from the value of n which gave the best fit. It was found to be zero in all the cases. With this value of n and using each of the three kinetic equations, E and A were calculated for all the TG curves and the correlation coefficient was also determined in each case.

Tables 2-6 give the values of E, A, and r, calculated using the three equations, for the thermal decomposition of the five resins at different heating rates. Table 7 gives the corresponding values of HC-434 for different sample masses.